JCI The Journal of Clinical Investigation

Similarities and differences between the immunopathogenesis of COVID-19-related pediatric inflammatory multisystem syndrome and Kawasaki disease

Ana Esteve-Sole, … , Iolanda Jordan, Laia Alsina

J Clin Invest. 2021. https://doi.org/10.1172/JCI144554.

Research In-Press Preview COVID-19 Immunology

Graphical abstract

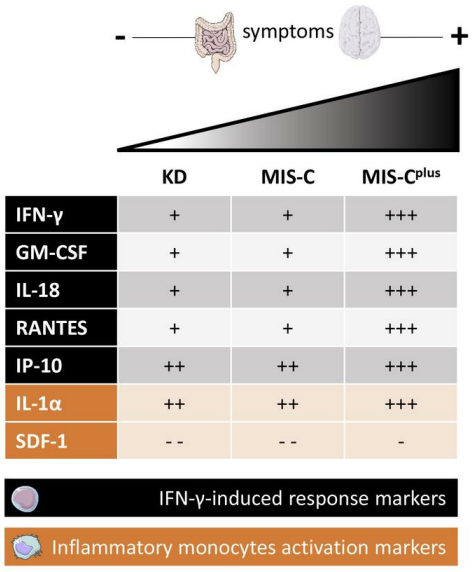

Similarities and differences between the immunopathogenesis of COVID-19-related pediatric inflammatory multisystem syndrome and Kawasaki disease

Ana Esteve-Sole*[1,2,3], Jordi Anton*[3-5], Rosa Maria Pino-Ramirez[6], Judith Sanchez-Manubens[3,5,7], Victoria Fumadó[3,4,8], Claudia Fortuny[3,4,8,9,10], María Rios-Barnes[8], Joan Sanchez-de-Toledo[3,11,12], Mónica Girona-Alarcón[13], Juan Manuel Mosquera[3,5], Silvia Ricart[4,6], Cristian Launes[3,4,6,9], Mariona Fernández de Sevilla[6,9], Cristina Jou[3,14,15,], Carmen Muñoz-Almagro[3,9,16,17], Eva González-Roca[18,19], Andrea Vergara[18,20], Jorge Carrillo[21], Manel Juan[2,4,19], Daniel Cuadras[3,22], Antoni Noguera-Julian[3,4,8,9,10], Iolanda Jordan[3,4,9, 13,]**Laia Alsina[1-4]****

***Authors contributed equally to the work

****Authors share senior co-authorship

Correspondence to:

Laia Alsina, Hospital Sant Joan de Déu (Avinguda Sant Joan de Déu, 2, Esplugues del Llobregat, Barcelona, 08950), Tel +34932804000, ext 71712 (lalsina@sjdhospitalbarcelona.org)
Ana Esteve-Sole Hospital Sant Joan de Déu (Avinguda Sant Joan de Déu, 2, Esplugues del Llobregat, Barcelona, 08950), Tel +34932804000, ext 71712 (aesteves@fsjd.org)

1. Allergy and Clinical Immunology Department, Hospital Sant Joan de Déu (HSJD), Barcelona, Spain
2. Clinical Immunology Unit, HSJD-Hospital Clínic de Barcelona (HCB), Barcelona, Spain.
3. Institut de Recerca Sant Joan de Déu, Barcelona, Spain.
4. Universitat de Barcelona, Barcelona, Spain.
5. Pediatric Rheumatology Department, HSJD, Barcelona, Spain.
6. Pediatrics Department, HSJD, Barcelona, Spain.
7. Pediatric Rheumatology Department, Hospital Parc Tauli, Sabadell, Spain.

8. Infectious Diseases Department, HSJD, Barcelona, Spain.

9. CIBER of Epidemiology and Public Health, Madrid, Spain

10. Translational Research Network in Paediatric Infectious Diseases (RITIP); Madrid, Spain

11. Cardiology Department, HSJD, Barcelona, Spain.

12. Department of Critical Care Medicine, University of Pittsburgh, Pittsburgh, USA

13. Pediatric Intensive Care Unit, HSJD, Barcelona, Spain.

14. Pathology Department and Biobank, HSJD, Barcelona, Spain.

15. Center for the Biomedical Research on Rare Diseases (CIBERER), ISCIII, Madrid, Spain

16. Department of Medicine. Universitat Internacional de Catalunya, Barcelona, Spain.

17. Molecular Microbiology Department, HSJD, Barcelona, Spain.

18. Molecular Biology Core, CDB, HCB-IDIBAPS, Barcelona, Spain.

19. Department of Immunology-CDB, HCB-IDIBAPS, Barcelona, Spain.

20. Microbiology Department, CDB, HCB, Barcelona, Spain.

21. IrsiCaixa AIDS Research Institute. Hospital Germans Trias i Pujol, Badalona, Catalonia, Spain.

22. Statistical Department. Fundació Sant Joan de Déu, Barcelona, Spain.

The authors declare that they have no conflicts of interest.

Abstract:

Multisystem inflammatory syndrome associated with the SARS-CoV-2 pandemic has recently been described in children (MIS-C), partially overlapping with Kawasaki disease (KD). We hypothesized that: 1) MIS-C and pre-pandemic KD cytokine profiles may be unique and justify the clinical differences observed; 2) SARS-CoV-2-specific immune complexes (IC) may explain the immunopathology of MIS-C. Seventy-four children were included: 14 MIS-C; 9 patients with positive SARS-CoV-2-PCR without MIS-C (COVID); 14 pre-pandemic KD and 37 healthy controls (HC). Thirty-four circulating cytokines were quantified in pre-treatment serum or plasma samples and the presence of circulating SARS-CoV-2 IC was evaluated in MIS-C patients. Compared to HC, MIS-C and KD groups showed most cytokines to be significantly elevated, with IFN-γ-induced response markers (including IFN-γ, IL-18, IP-10) and inflammatory monocytes activation markers (including MCP-1, IL-1α, IL-1RA) being the main triggers of inflammation. With linear discriminant analysis, MIS-C and KD profiles overlapped; however, a subgroup of MIS-C patients (MIS-C^{plus}) differentiated from the remaining MIS-C patients in IFN-γ, IL-18, GM-CSF, RANTES, IP-10, IL-1α and SDF-1 and incipient signs of macrophagic activation syndrome. Circulating SARS-CoV-2-IC were not detected in MIS-C patients. Our findings suggest a major role of IFN-γ in the pathogenesis of MIS-C, which may be relevant for therapeutic management.

Graphical Abstract

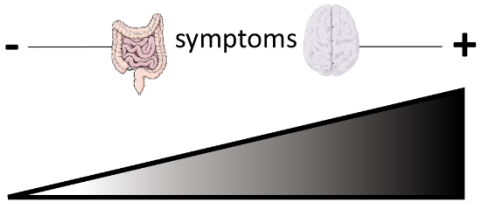

	KD	MIS-C	MIS-C^{plus}
IFN-γ	+	+	+++
GM-CSF	+	+	+++
IL-18	+	+	+++
RANTES	+	+	+++
IP-10	++	++	+++
IL-1α	++	++	+++
SDF-1	- -	- -	-

IFN-γ-induced response markers

Inflammatory monocytes activation markers

Introduction

Late in April 2020, a multisystem inflammatory syndrome temporary associated with SARS-CoV-2 was described in children (MIS-C) (1), occurring 4-6 weeks after the infectious peak (2–6). The diagnostic criteria for this entity were developed by health agencies based on the initial cases described (7–9), lacking specific biomarkers (7–10).

MIS-C shares common features with Kawasaki disease (KD) and patients were initially treated following KD recommendations. However, there are notable differences, with the incidence of MISC being higher (2), and patients present with 1) older age, 2) increased gastrointestinal and neurological signs, 3) higher incidence of myocarditis and cardiac involvement and 4) increased ferritin, leukopenia, lymphopenia and thrombocytopenia (2–5, 11, 12). Godfred-Cato *et al* (13) recently identified 3 non-exclusive categories of patients within MIS-C: Class 1 with increased gastrointestinal and neurological manifestations, also named "True" or classic MIS-C (10), Class 2 or "acute COVID", most of them with positive SARS-CoV-2 PCR and negative serology; and Class 3 or "KD-like" (10), with a phenotype similar to pre-pandemic KD.

The underlying mechanism of MIS-C remains elusive. Currently, KD is categorized as a vasculitis (14) and it is considered to result from the exposure of a genetically predisposed child to an unidentified, possibly infectious agent. This interaction may generate a disbalance in the immune system, with increased Th1/Th17-related immunity and a Treg/Th17 disbalance. This would lead to increased production of inflammatory cytokines and chemokines such as TNF-α, IL-1, IL-2, IL-6, IL-8, MCP-1 and GM-CSF, causing macrophage and neutrophil hyperactivation (15). SARS-CoV-2 is a single-stranded RNA virus (16) and infections caused by RNA viruses have been linked to KD (11). Type III hypersensitivity reactions may explain part of the pathogenesis of KD by immune complexes' (IC), since causal association has been reported (11, 17, 18). Of note, deposited IC were detected in the endothelium of an adult patient with SARS-CoV-2-related vasculitis 18 days after an infection confirmed by polymerase chain reaction (PCR) (19).

We hypothesized that: 1) cytokine profiles observed in MIS-C and pre-pandemic KD patients may be unique; and 2) SARS-CoV-2 specific IC may explain the immunopathology of MIS-C.

Results

Cohort description

Seventy-four children were studied: 14 MIS-C (median age 2.9 years, range 0.3-14); 14 pre-pandemic KD (median age 2 years, range 0.5-6); 9 COVID patients with positive SARS-CoV-2 nasopharyngeal reverse transcriptase (RT)-PCR (mean age 10 years, range 0.1-14) and 37 healthy controls (HC, median age 5 years, range 1-11; among the latter, 16/37 HC patients had both serum and plasma samples collected in parallel, adding up to a total of 53 HC samples). The clinical characteristics of 12 out of the 14 MIS-C patients of this cohort have previously been described by Pino et al (6), showing: increased gastrointestinal and neurological symptoms, increased lymphopenia and thrombopenia, and decreased neutrophilia, with statistically significant differences compared with KD patients (**Table 1 and 2, Supplementary Tables 1 and 2**). Eight of the 14 MIS-C patients had SARS-CoV-2 specific IgG, 6 of whom were also positive for IgA and none to IgM (**Figure 1**). MIS-C patients were treated according to KD recommendations in the absence of specific recommendations at that time. The COVID patients included had a mild disease course; seven out of nine had positive IgG.

Cytokine profiling

Cytokine profiling was performed in serum or plasma samples prior to immunomodulatory treatment (except in 2 patients who received immunoglobulins 2 days before blood extraction) and at a median time from disease onset of 5.50, 4.50 and 1.50 days for MIS-C, KD and COVID patients, respectively. Plasma and serum cytokine levels were normalized to plasma and serum HC samples to Log2-fold-change (Log2FC), to avoid sample-source dependent differences **(Supplementary methods, Supplementary Figure 1)** and were compared across groups (**Supplementary Table 3** and **Supplementary Figure 2)**.

In order to compare the 34-cytokine profile across groups, we performed an unsupervised multiparametric analysis through principal component analysis (PCA) (**Figure 2A**). In PCA,

principal components (PC) explain the maximum variance among all individuals. After PCA plotting of PC1 and PC2, HC and mild-COVID patients were grouped in the same area, being still distinguishable, but apart from the MIS-C and KD groups, which partially overlapped. We identified 13 cytokines with a higher impact in the observed variance (**Figure 2B**). Comparison of cytokine levels between KD/MIS-C and HC showed statistically significant differences in all cytokines but IL-2, TNF-α, MIP-1α, MIP-1β and IL-22 (**Supplementary Table 3; Supplementary Figure 2**).

Although mild-COVID patients were zoned in the same area as HC, they were not superimposed. Circulating cytokine levels of mild-COVID and HC were statistically significantly different in 17/34 cytokines measured, including IFN-γ, IP-10, IL-1α, GM-CSF, GRO-α and SDF-1 of the selected PCA cytokines (**Figure 2B).** However, their increase in mild-COVID patients was lower than that observed in MIS-C or KD patients.

We performed a supervised analysis through linear discriminant analysis (LDA) based on selected PC1 and PC2 13 cytokines, to explore if they were sufficient to create a model that could distinguish between the different groups, in particular MIS-C and KD. LDA generated 3 Canonical variants (Can1-3), explaining the maximum variability between groups: Can1 and Can2 were able to visually differentiate HC and COVID from the other groups, but not KD from MIS-C (**Figure 2C**). Testing the model using the leave-one-out cross-validation was useful for distinguishing between HC, COVID and MIS-C+KD, but not between KD and MIS-C (**Figure 3**).

Visualization of Can2 *vs* Can3 showed that 5 patients with MIS-C (MIS-C^{plus}) presented a unique pattern (**Figure 2D**). Of the 13 cytokines selected to build the LDA model, IFN-γ, IL-18, GM-CSF, RANTES, IP-10, IL-1α and SDF-1 statistically significantly differentiated MIS-C^{plus} patients from the remaining MIS-C patients (**Supplementary Table 4**; **Figure 2E**). The absolute values of these cytokines are shown in **Figure 4.** Specifically, the median circulating IFN-γ levels in MIS-C^{plus} patients were 114.9pg/ml (range 44.4pg/ml to 259.5pg/ml; **Figure 4**), higher than in the remaining MIS-C patients (median of 10pg/ml), KD patients (median of 19.9pg/ml) and mild-

COVID patients (7.5pg/ml) (**Figure 4**).-While only 33% of all MIS-C patients were classified as MIS-C after leave-one-out cross validation, 80% of MIS-C^{plus} patients were classified as MIS-C (**Figure 3**).

MIS-C^{plus} patients tended to have increased organ systems involvement compared to MIS-C (median: 5 (2-6) *vs* 3 (1-6), respectively, p: 0.08; **Supplementary Table 5**). Concretely, MIS-C^{plus} patients presented with increased neurological symptoms compared with the remaining MIS-C patients (80% *vs* 11%, p: 0.023, **Supplementary Table 5**). SARS-CoV-2 RT-PCR testing in stool was performed in 80% of MIS-C^{plus} patients compared to only 2 of the 9 remaining MIS-C patients, suggesting an increased severity of gastrointestinal symptoms. In addition, specific-SARS-CoV-2 IgA was positive or indeterminate in 80% MIS-C^{plus} patients compared to 37.5% of the remaining MIS-C patients (p: 0.21). Although not reaching statistical significance, MIS-C^{plus} patients displayed lower platelet levels (median of 170,000 *vs* 373,000 platelets/mm^3; p: 0.08) and a higher frequency of altered procalcitonin (100% *vs* 55.6%; p: 0.08) and ferritin values (100% *vs* 55.6%; p: 0.08)(**Supplementary Table 6**).

Detection of SARS-CoV-2 immune complexes

SARS-CoV-2 IC were determined by quantifying SARS-CoV-2 RNA pre- and post-immunoprecipitation for IgA and IgG, chosen because specific SARS-CoV-2 IgG and IgA were reported in MIS-C patients **(Figure 1)** (21) and because of their reported role in KD IC-mediated pathogenesis (17). We performed SARS-CoV-2 real-time RT-PCR in 1) pre- treated serum, 2) IgG-immunoprecipitation (IP), 3) IgA-IP, 4) IgG-IgA free serum in MIS-C patients and in one positive and negative control. We did not detect circulating SARS-CoV-2 RNA nor SARS-CoV-2 IC in any MIS-C patients **(Supplementary Figure 3).**

Discussion:

SARS-CoV-2 seemed to have spared children until the appearance of MIS-C in pediatric patients, which at first was classified as a "Kawasaki-like" manifestation of the infection (1). In order to better understand the similarities and differences between these two entities, we evaluated circulating cytokine levels in pediatric patients with MIS-C, pre-pandemic KD and mild-COVID and the presence of SARS-CoV-2 of IC in MIS-C patients. Our findings suggest that: 1) IFN-γ and inflammatory monocytes are the main drivers of inflammation in MIS-C patients and 2) MIS-C patients can be subdivided into two groups: one similar to KD in terms of clinical and cytokine profiles (described as Class3 (13) or KD-like (10)), and one described as Class1 (13), "True" or classic MIS-C (10), with more severe inflammation (especially IFN-γ-related) and increased neurological and gastrointestinal manifestations. Circulating SARS-CoV-2 IC could not be identified in MIS-C patients.

Clinical and routine laboratory parameters of MIS-C patients as well as specific SARS-CoV-2 serology results were in accordance with other published reports, in which specific SARS-CoV-2 IgG antibodies have been observed before day 10 of symptoms' onset (2–4, 21–23). Circulating cytokine determination included 34 cytokines and chemokines, covering most of the cytokines described as being elevated in MIS-C patients (5, 22, 24–26). After PCA analysis, we selected 13 cytokines that explained most of the observed variance across individuals. Selected cytokines in PC1 (64.5% of variance) were enriched in IFN-γ-related cytokines while those in PC2 (8.8% of the variance) were enriched in IL-1 and inflammatory monocyte pathways (**Figure 2B)**, suggesting a principal role of these cytokines in the inflammation observed in KD and MIS-C. Activation of inflammatory monocytes ($CD16^+$) has already been described in MIS-C patients (22, 24) as well as in severe-adult-SARS-CoV-2 patients (18). Besides, moderate increase in circulating cytokine levels observed in mild-COVID patients was in accordance with previous reports (22, 24).

Previous reports have also evaluated circulating cytokine profiles in MIS-C patients (5, 22, 24, 26, 27), two of which included KD patients (5, 26). Although a similar approach was used, the

cohorts are not fully comparable. There were differences in the definition of HC/COVID patients, and the time from disease onset to cytokine testing was only specified in one study (24), being uncertain whether it was prior to immunomodulatory treatment. Despite these differences, reported evidence agrees that MIS-C patients display an increase of inflammatory cytokines including IFN-γ (25), IL-10 (24–26), IL-6 (5, 25, 26), IL-8 (24, 25), CXCL10 (22, 24, 28), MIP-1α, MIP-1β (22), TNF-α (24, 25) and IL-17 (23, 32), in MIS-C patients compared to HC and other COVID pediatric patients. These results are in accordance with our observations (**Supplementary Figure 2; Supplementary Table 3**). In addition, CXCL9 (26) and IL-2RA (24, 26) were also found to be increased in MIS-C patients.

Consiglio *et al* (5) compared MIS-C patients from Italy and Sweden with pre-pandemic Italian KD patients. They performed PCA analysis of 180 proteins in plasma, finding that a subgroup of MIS-C patients overlapped with KD patients and another clearly differentiated. They found an especially large increase in IL-17 in KD patients in comparison with HC and COVID patients, which was not observed in MIS-C patients. We and others (22, 24) have observed a marked increase of circulating IL-17 levels in KD patients but also in MIS-C patients, though to a lesser extent in the latter (1.15 *vs* 1.50 median Log2FC in MIS-C and KD patients, respectively in relation to HC; 6.84pg/ml *vs* 13.63pg/ml *vs* 1.40pg/ml median quantitative levels in MIS-C, KD and HC respectively, **Supplementary Table 3, Supplementary Figure 4**). These differences may be ascribed to a different behavior of the Swedish cohort, taking into account the medRxiv version of the paper (28).

The marked increase in circulating levels of IFN-γ, IL-18 IP-10 in MIS-C^{plus} patients in comparison with other MIS-C and KD patients, led to suspicion of a possible relationship with macrophage activation syndrome (MAS) (29–31). Indeed, the presence of MAS was plausible in one patient (MIS-C^{plus}, ID11, **Supplementary Table 2**). These cytokines are also known to be increased in severe COVID patients (18). Elevation of circulating IFN-γ is a hallmark of hemophagocytic syndromes (HLH) including MAS, and its determination in serum in different studies has shown varying results. IFN-γ is normally undetectable in healthy controls (32).

Increased levels of IFN-γ have been reported in viral infections (mean of 18.9pg/ml; range 7.7-33.4pg/ml) (33) and specially high serum levels are detected in patients with suspected primary HLH (fulfilling HLH-2004 diagnostic criteria (34), below 10 years of age, with or without confirmed genetic diagnosis)(mean of 1807pg/ml(range 147.6 to >5000pg/ml) (33) and 905pg/ml, (95% confidence interval: 530.7–1280.6 pg/ml) (35). Patients with MAS associated with systemic juvenile idiopathic arthritis showed mean serum IFN-γ levels of 15.4pg/ml (5.1-52.6pg/ml interquartile range), although using a different quantification technique in comparison with the other two studies (36). Thus MIS-C^{plus} median IFN-γ circulating levels were higher than in viral infections and MAS, but lower than in suspected primary HLH, therefore suggesting that circulating IFN-γ levels in MIS-C^{plus} cannot only be ascribed to a viral infection but rather may represent a mechanism of disease.

Negative detection of IC do not rule out their possible role in the immunopathogenesis of MIS-C and this might be explained by two hypotheses: 1) the IC may already be deposited in the endothelium and thus are not detectable in serum/plasma or 2) the pathogenesis may be mediated by direct infection of the endothelium. IC have been described in vascular tissue of a SARS-CoV-2 patient with vasculitis (19) and SARS-CoV-2 viral particles have been observed inside the endothelium in pediatric patients with SARS-CoV-2 related chill-blains (37). The absence of vascular tissue biopsies limits further exploration of this hypothesis.

Our study presents both strengths and limitations. It is of note that most samples were collected within the first week after the beginning of the symptoms and prior to any immunomodulatory treatment except in only 2/74 children, who were still clinically active and presented an inflammatory profile. In addition, the cytokine profile was normalized to plasma and serum of age-matched pediatric HC, enabling a more robust comparison between different groups and interpretation of results. On the other hand, the cohorts are modest in size, but large enough observe differences. Also, we had limited access to different types of samples, including peripheral blood mononuclear cells and tissue biopsies, that could have been useful for evaluation of T cell immunity and monocytes' phenotyping.

In summary, our results replicate the routine-clinical laboratory differences observed between KD and MIS-C (2, 5, 26). In our cohort, IFN-γ related cytokines, and cytokines related to IL-1 and inflammatory monocytes were the main contributors to acute inflammation both in MIS-C and KD patients, which mostly overlapped. A subgroup of MIS-C patients (MIS-C^{plus}) showed a more pronounced increase in IFN-γ-related cytokines and a trend a towards more severe multisystemic disorder, resembling the Class1 (13) also named "True" or classic MIS-C (10) (MIS-C^{plus} patients) *vs* Class3 or "KD-like" (10) (remaining MIS-C patients) classification of Godfred-Cato (13). We speculate that the differential gastrointestinal involvement by SARS-CoV-2 infection may contribute to the differential cytokine profile observed in MIS-C^{plus} compared to KD patients. Our findings can may be useful for the development of targeted treatments to optimize patient management and, ultimately reduce the estimated mortality of 2% in patients with MIS-C (4).

Methods:

From April 23rd (4 weeks after the exponential increase of COVID-19 cases in our area and schools shut-down) to June 5th 2020, 14 patients with MIS-C (according to WHO (7) or Royal College criteria (8), 9 pediatric patients with positive PCR to SARS-CoV-2 without MIS-C (COVID) and 37 pediatric healthy controls (HC) with negative SARS-CoV-2 PCR and serology were recruited. Fourteen patients with pre-pandemic Kawasaki disease (KD), according to AHA criteria (38), were also recruited between 2016 and 2019. Patient definition and inclusion criteria are defined in **Supplementary Methods**.

This was a cross-sectional study. Patient's blood samples were drawn between day 1 and day 10 of disease evolution (with the exception of one KD patient in whom disease onset had been 14 days but who still presented increased C reactive protein levels) for routine laboratory analysis, quantification of 34 different circulating cytokines and evaluation of the presence of circulating SARS-CoV-2 IC (only in patients with MIS-C). Sampling was performed before the administration of immunomodulatory treatment (intravenous immunoglobulin (IVIG), steroids, tocilizumab, anakinra) in all but two patients who received IVIG two days before the extraction. None of the patients had preexisting conditions, except for one COVID patient in remission of an acute lymphocytic leukemia after stem cell transplantation in 2017.

SARS-CoV-2 infection determination:

Real-time PCR (RT-PCR) for nasopharyngeal/stool samples

Viral RNA extraction was performed with NucliSENS easyMAG (BioMerieux Laboratories) or MagMAX™ Viral/Pathogen Nucleic Acid Isolation Kit" (Thermo Fisher Scientific) following the manufacturer's instructions. RT-PCR was performed with the COVID-19 Plus RealAmp Kit (Genefinder laboratories) for detection of the RdRp, E, N viral genes and the human RnaseP gene as internal control.

SARS-CoV-2 serology

IgG, IgA and IgM antibodies specific to SARS-CoV-2 were determined using a Luminex system against the receptor-binding domain of the spike glycoprotein of SARS-CoV-2 as reported (39). Briefly, 10µl of plasma were incubated with antigen-coupled beads for two hours at room temperature (RT) with agitation. Plates were then washed three times and incubated with biotinylated secondary antibody (IgM, IgA or IgG, Sigma-Aldrich, St. Louis, MO, USA) for 45 minutes at RT with agitation. Plates were washed three times and streptavidin-R-phycoerythrin (Sigma-Aldrich) was added for 30 minutes at RT with agitation. Plates were washed three times and beads were resuspended in phosphate buffered saline (PBS, Roche Diagnostics, Barcelona, Spain). Plates were read using a Luminex xMAP® 100 analyzer (Waltham, MA, USA).

Cytokine quantification

Cytokine determination was assessed with the Luminex System (Procartaplex, Thermofisher, Waltham, MA, USA) performed in serum or plasma of patients the following the manufacturer's instructions. The cytokines detected included: Eotaxin/CCL11; GM-CSF; GRO alpha/CXCL1; IFN alpha; IFN gamma; IL-1 beta; IL-1 alpha; IL-1RA; IL-2; IL-4; IL-5; IL-6; IL-7; IL-8/CXCL8; IL-9; IL-10; IL-12 p70; IL-13; IL-15; IL-17A; IL-18; IL-21; IL-22; IL-23; IL-27; IL-31; IP-10/CXCL10; MCP-1/CCL2; MIP-1 alpha/CCL3; MIP-1 beta/CCL4; RANTES/CCL5; SDF1 alpha/CXCL12; TNF alpha; TNF beta/LTA. Plates were read using a Luminex xMAP® 100 analyzer.

SARS-CoV-2 immune complexes evaluation

Specific viral IC against SARS-CoV-2 were detected adapting a previous protocol used to detect hepatitis C virus IC (40, 41). This consisted of the immunoprecipitation of IgG or IgA followed by subsequent determination of viral load with quantitative PCR. Specifically, for each sample, 25µl of 10mg/ml streptavidin magnetic beads (Thermo Fisher Scientific, Waltham, MA, USA) were incubated with 5µg of IgG-biotin (Sigma-Aldrich) or IgA-biotin (Sigma-Aldrich) for each sample for 30 minutes at RT with orbital agitation. After two washes with PBS bovine serum albumin (BSA) (0.05% Sigma-Aldrich), magnetic beads were resuspended to the original volume

with PBS-BSA. 25µl of magnetic beads coupled with IgG were incubated with 100µl of serum from the patients for 30 minutes at RT with orbital agitation. Magnetic separation between the beads and the supernatant was performed. The process was repeated with resulting SN and IgA coupled magnetic beads. SARS-CoV-2 virus was measured from pre-treated serum, IgG immunoprecipitated fraction, IgA immunoprecipitated fraction and supernatant fraction by quantitative PCR.

For the detection of nucleid acid from SARS-CoV-2 in serum samples, RNA was isolated with the "MagMAX™ Viral/Pathogen Nucleic Acid Isolation Kit" (Thermo Fisher Scientific), following the manufacturer's instructions. A multiplex real-time RT-PCR (TaqPath™ COVID-19 CE-IVD RT-PCR Kit" from ThermoFisher Scientific) was performed in an Applied Biosystems® 7500 Fast Real-Time PCR System (ThemoFisher Scientific) to detect the genes encoding for SARS-CoV-2 ORF1ab, N Protein and S Protein. An internal control (MS2 Phage Control) was included before RNA extraction to control the procedure. The assay included a positive and negative control.

Routine hematological and biochemical analysis

A broad battery of routine laboratory parameters including hemogram, erythrocytes sedimentation rate (ESR) mm/hour, D-dimer, procalcitonin (PCT), C-reactive protein (CRP), ferritin, N-terminal pro-brain natriuretic peptide (NTPro-BNP), sodium (Na), lactate dehydrogenase (LDH) and albumin were studied within the routine hospital care.

Statistics

For the analysis of clinical data, the Mann-Whitney test was performed to compare numerical variables between two groups and the Chi-square test was used to compare categorical variables between two groups.

For the analysis of cytokine levels, we used relative changes in the fluorescence intensities, as recommended (42). Since we had both plasma and serum samples from patients (**Supplementary Table 7**) and the effect of matrix from plasma and serum may affect the results (42), data from

serum samples were normalized with the mean of serum samples from healthy controls, and data from plasma samples were normalized with the mean of plasma samples from healthy controls to minimize this effect. After normalization with HC, Log2 was applied to all samples to calculate Log2 Fold Change (Log2FC) of all the samples compared to the mean of the healthy control group (22) (**Supplementary Figure 1**).

For principal component analysis (PCA) we used the single value decomposition without data scaling since data were already normalized. PCA and heatmap analysis was performed using the online tool ClustVis (43). Linear Discriminant Analysis was performed on the normalized data using R package Candisc (Discriminant and Canonical Correlation Analysis. R package version 0.8; 10).

The Kruskal-Wallis test was performed for all the cytokines, using Bonferroni correction for comparisons of all the samples. Pair-wise comparisons using the Mann-Whitney test were only performed when the Kruskal-Wallis test was significant after Bonferroni correction. Mann-Whitney test results were corrected for multiple comparisons (4 groups, 6 comparisons) with Bonferroni Correction. Statistical tests results were considered significant when $p<0.05$. To compare the circulating cytokine levels of MIS-C^{plus} patients with the remaining MIS-C and KD patients, Bonferroni correction was not performed due to sample size limitation as previously reported (25). Taking into account the sample size, changes reported as statistically significant should be interpreted as indicative of the direction of change in biological signals.

The statistical analyses and graphical representation of the data were made with SPSS 22 (IBM, Armonk, NY, USA), Prism8 (Graphpad, Software, San Diego, CA USA), online tool ClustVis (43) and R 3.6 (Foundation for Statistical Computing, Vienna, Austria).

Study approval:

This study was carried out in accordance with the recommendations of the *Ley General de Sanidad (25/4/1986) Art. 10*. The protocol was approved by the Ethics Committee of Hospital Sant Joan de Déu (PIC-58-60). Parents and children over the age of 12 years signed the informed consent or assent, in compliance with current legislation.

Author contributions

LA, IJ, AES, JA, MJ, VF and CFG conceptualized and designed the research. AES Performed immunologic studies. AV, EGR, MC and MJ performed SARS-CoV-2 detection. LA, AES, RMPR, IJ analyzed and interpreted data. RMPR, JSM, VF, CFG, MR, JSdT, MGA, JMM, SR, CL, MFdS, CJ, CMA, IJ provided patient material and clinical data and participated in discussion of the results. AES, JA, RMPR, SR, ANJ, DC, IJ and LA discussed the integration of the data. AES prepared the figures. AES and LA wrote the manuscript.

AES and JA share co-authorship since AES was responsible for the immunologic studies while JA was in charge of patient recruitment and clinical evaluation; AES is first co-author because of her role in manuscript writing.

All authors have read the manuscript, contributed to manuscript revision, and approved the submitted version.

Acknowledgements

The authors especially thank the participants of the study and all the people involved in the care of the patients.

We are indebted to the "Biobanc de l'Hospital Infantil Sant Joan de Déu per a la Investigació" integrated in the Spanish Biobank Network of ISCIII for the sample and data procurement.

This study was supported by the projects PI15/01094, PFIS0200 (AC16/00025), PI18/00223 and FI19/00208 to LA, integrated in the Plan Nacional de I+D+I and cofinanced by the ISCIII – Subdirección General de Evaluación y Formento de la Investigación Sanitaria –FEDER;PERIS, Departament de Salut, Generalitat de Catalunya (SLT006/17/00199 to LA); 2017 Leonardo Grant for Researchers and Cultural Creators, BBVA Foundation to LA; 2017 Beca de Investigación de la SEICAP to LA; WINDBIOME grant from Daniel Bravo Fundation and 2018 SERPE grant from SERP. This work was also partially funded by Stavros Niarchos Foundation (SNF), Banco Santander and other private donors of "KidsCorona platform" from Hospital Sant Joan de Déu and by CELLNEX TELECOM (5234-20/CPO42837).

References:

1. Riphagen S, Gomez X, Gonzalez-Martinez C, Wilkinson N, Theocharis P. Hyperinflammatory shock in children during COVID-19 pandemic. *Lancet* 2020;395(10237):1607–1608.

2. Verdoni L, et al. An outbreak of severe Kawasaki-like disease at the Italian epicentre of the SARS-CoV-2 epidemic: an observational cohort study. *Lancet* 2020;6736(20):1–8.

3. European Centre for Disease Prevention and Control. *Paediatric inflammatory multisystem syndrome and SARS-CoV-2 infection in children*. Stockholm: 2020:

4. Feldstein LR, et al. Multisystem Inflammatory Syndrome in U.S. Children and Adolescents. *N Engl J Med* 2020;NEJMoa2021680.

5. Consiglio CR, et al. The Immunology of Multisystem Inflammatory Syndrome in Children with COVID-19. *Cell* [published online ahead of print: September 6, 2020];

6. Pino R, et al. Correspondence on: 'Paediatric multisystem inflammatory syndrome temporally associated with SARS-CoV-2 mimicking Kawasaki disease (Kawa-COVID-19): a multicentre cohort' by Pouletty et al . *Ann Rheum Dis* 2020;annrheumdis-2020-218538.

7. World Health Organization. *Multisystem inflammatory syndrome in children and adolescents temporally related to COVID-19*. 2020:

8. Royal College of Paediatrics and Child Health. *Guidance: Paediatric multisystem inflammatory syndrome temporally associated with COVID-19*. 2020:

9. Preparedness E. Emergency Preparedness and Response Multisystem In ammatory Syndrome in Children (MIS-C) Associated with Coronavirus Disease 2019. *CDCGOV* 2020;2019–2021.

10. Rowley AH, Shulman ST, Arditi M. Immune pathogenesis of COVID-19-related Multisystem Inflammatory Syndrome in Children (MIS-C).. *J Clin Invest* [published online ahead of print: 2020];

11. Burns JC, Glodé MP. Kawasaki syndrome. *Lancet* 2004;364(9433):533–544.

12. Cheung EW, et al. Multisystem Inflammatory Syndrome Related to COVID-19 in Previously Healthy Children and Adolescents in New York City. *JAMA* 2020;324(3):294.

13. Godfred-Cato S, et al. *Morbidity and Mortality Weekly Report Early Release / COVID-19-Associated Multisystem Inflammatory Syndrome in Children-United States, March-July 2020*. 2020:

14. Ozen S. EULAR/PReS endorsed consensus criteria for the classification of childhood vasculitides. *Ann Rheum Dis* 2005;65(7):936–941.

15. Takahashi K, Oharaseki T, Yokouchi Y. Update on etio and immunopathogenesis of Kawasaki disease. *Curr Opin Rheumatol* 2014;26(1):31–36.

16. Perez-Toledo M, et al. Serology confirms SARS-CoV-2 infection in PCR-negative children presenting with Paediatric Inflammatory Multi-System Syndrome. *medRxiv* 2020;2020.06.05.20123117.

17. Menikou S, Langford PR, Levin M. Kawasaki Disease: The Role of Immune Complexes Revisited. *Front Immunol* 2019;10(JUN).

18. Vabret N, et al. Immunology of COVID-19: current state of the science. *Immunity* 2020;52(6):910–941.

19. Roncati L, et al. Type 3 hypersensitivity in COVID-19 vasculitis.. *Clin Immunol* 2020;217:108487.

20. Huang K-J, et al. An interferon-g-related cytokine storm in SARS patients. *J Med Virol* 2005;75(2):185–194.

21. Weisberg SP, et al. Distinct antibody responses to SARS-CoV-2 in children and adults across the COVID-19 clinical spectrum. *Nat Immunol* [published online ahead of print: November 5, 2020];

22. Gruber CN, et al. Mapping Systemic Inflammation and Antibody Responses in Multisystem Inflammatory Syndrome in Children (MIS-C). *Cell* 2020;183(4):982-995.e14.

23. Jin Y, et al. Diagnostic value and dynamic variance of serum antibody in coronavirus disease 2019. *Int J Infect Dis* 2020;94:49–52.

24. Carter MJ, et al. Peripheral immunophenotypes in children with multisystem inflammatory syndrome associated with SARS-CoV-2 infection. *Nat Med* 2020;26(11):1701–1707.

25. Diorio C, et al. Multisystem inflammatory syndrome in children and COVID-19 are distinct

presentations of SARS-CoV-2. *J Clin Invest* [published online ahead of print: July 30, 2020];

26. Lee PY, et al. Distinct clinical and immunological features of SARS-COV-2-induced multisystem inflammatory syndrome in children. *J Clin Invest* [published online ahead of print: July 23, 2020];

27. Anderson EM, et al. SARS-CoV-2 antibody responses in children with MIS-C and mild and severe COVID-19. *J Pediatric Infect Dis Soc* [published online ahead of print: December 2, 2020];

28. Consiglio CR, et al. *The Immunology of Multisystem Inflammatory Syndrome in Children with COVID-19*. Cold Spring Harbor Laboratory Press; 2020:

29. Crayne CB, Albeituni S, Nichols KE, Cron RQ. The immunology of macrophage activation syndrome. *Front Immunol* 2019;10(FEB):1–11.

30. Jinkawa A, et al. Cytokine profile of macrophage activation syndrome associated with Kawasaki disease. *Cytokine* 2019;119:52–56.

31. Lee W-I, et al. Immune defects in active mycobacterial diseases in patients with primary immunodeficiency diseases (PIDs).. *J Formos Med Assoc* 2011;110(12):750–8.

32. Fieschi C, et al. High levels of interferon gamma in the plasma of children with complete interferon gamma receptor deficiency.. *Pediatrics* 2001;107(4):E48.

33. Tang Y, et al. Early diagnostic and prognostic significance of a specific Th1/Th2 cytokine pattern in children with haemophagocytic syndrome. *Br J Haematol* 2008;143(1):84–91.

34. Henter JI, et al. HLH-2004: Diagnostic and therapeutic guidelines for hemophagocytic lymphohistiocytosis. *Pediatr Blood Cancer* 2007;48(2):124–131.

35. Chen Y, et al. Comparison of Th1/Th2 cytokine profiles between primary and secondary haemophagocytic lymphohistiocytosis. *Ital J Pediatr* 2016;42(1).

36. Bracaglia C, et al. Elevated circulating levels of interferon-γ and interferon-γ-induced chemokines characterize patients with macrophage activation syndrome complicating systemic juvenile idiopathic arthritis. *Ann Rheum Dis* 2017;76(1):166–172.

37. Colmenero I, et al. SARS‐CoV‐2 endothelial infection causes COVID‐19 chilblains: histopathological, immunohistochemical and ultraestructural study of 7 paediatric cases. *Br J*

Dermatol 2020;bjd.19327.

38. McCrindle BW, et al. Diagnosis, Treatment, and Long-Term Management of Kawasaki Disease: A Scientific Statement for Health Professionals From the American Heart Association. *Circulation* 2017;135(17).

39. Garcia-Basteiro AL, et al. Seroprevalence of antibodies against SARS-CoV-2 among health care workers in a large Spanish reference hospital. *Nat Commun* 2020;11(1):3500.

40. Morita T, et al. Detection of hepatitis C virus RNA in circulating immune complexes by RT-PCR.. *Hepatogastroenterology* 1996;43(9):582–5.

41. Aiyama T, et al. Sequence Analysis of Hypervariable Region of Hepatitis C Virus (HeV) Associated with Immune Complex in Patients with Chronic HCV Infection. *J Infect Dis* 1996;174(6):1316–1319.

42. Rosenberg-Hasson Y, Hansmann L, Liedtke M, Herschmann I, Maecker HT. Effects of serum and plasma matrices on multiplex immunoassays. *Immunol Res* 2014;58(2–3):224–233.

43. Metsalu T, Vilo J. ClustVis: a web tool for visualizing clustering of multivariate data using Principal Component Analysis and heatmap. *Web Serv issue Publ online* 2015;43.

44. Friendly M, Fox J. Package "candisc" Type Package Title Visualizing Generalized Canonical Discriminant and Canonical Correlation Analysis. *CRAN* [published online ahead of print: 2017];

45. Kanegaye JT, et al. Recognition of a Kawasaki disease shock syndrome. *Pediatrics* 2009;123(5).

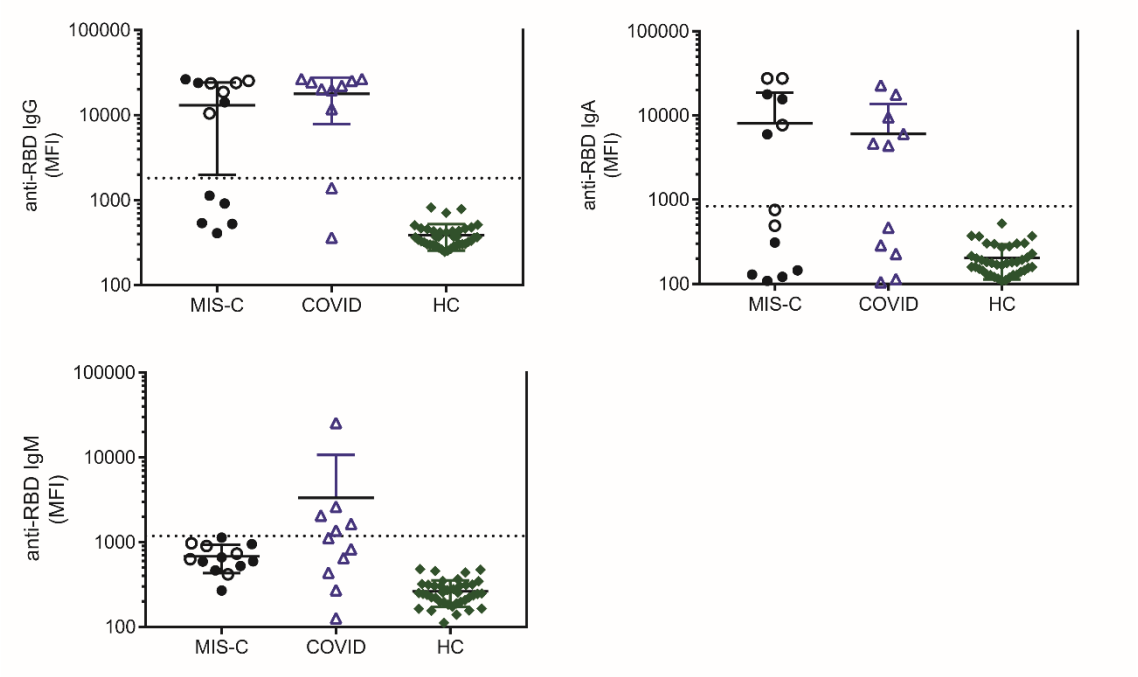

Figure 1. SARS-CoV-2 specific immunoglobulin detection. Determination of IgG, IgA and IgM anti-RBD domain SARS-CoV-2 spike protein. Open symbols represent patients with positive PCR in nasal swab or stools. Dotted line represent threshold for positivity.

MFI: mean fluorescence intensity; MIS-C: multi inflammatory syndrome in children (n=13). COVID: pediatric patients with mild COVID-19 disease without MIS-C (n=9); HC: healthy controls (n=37, 53 samples).

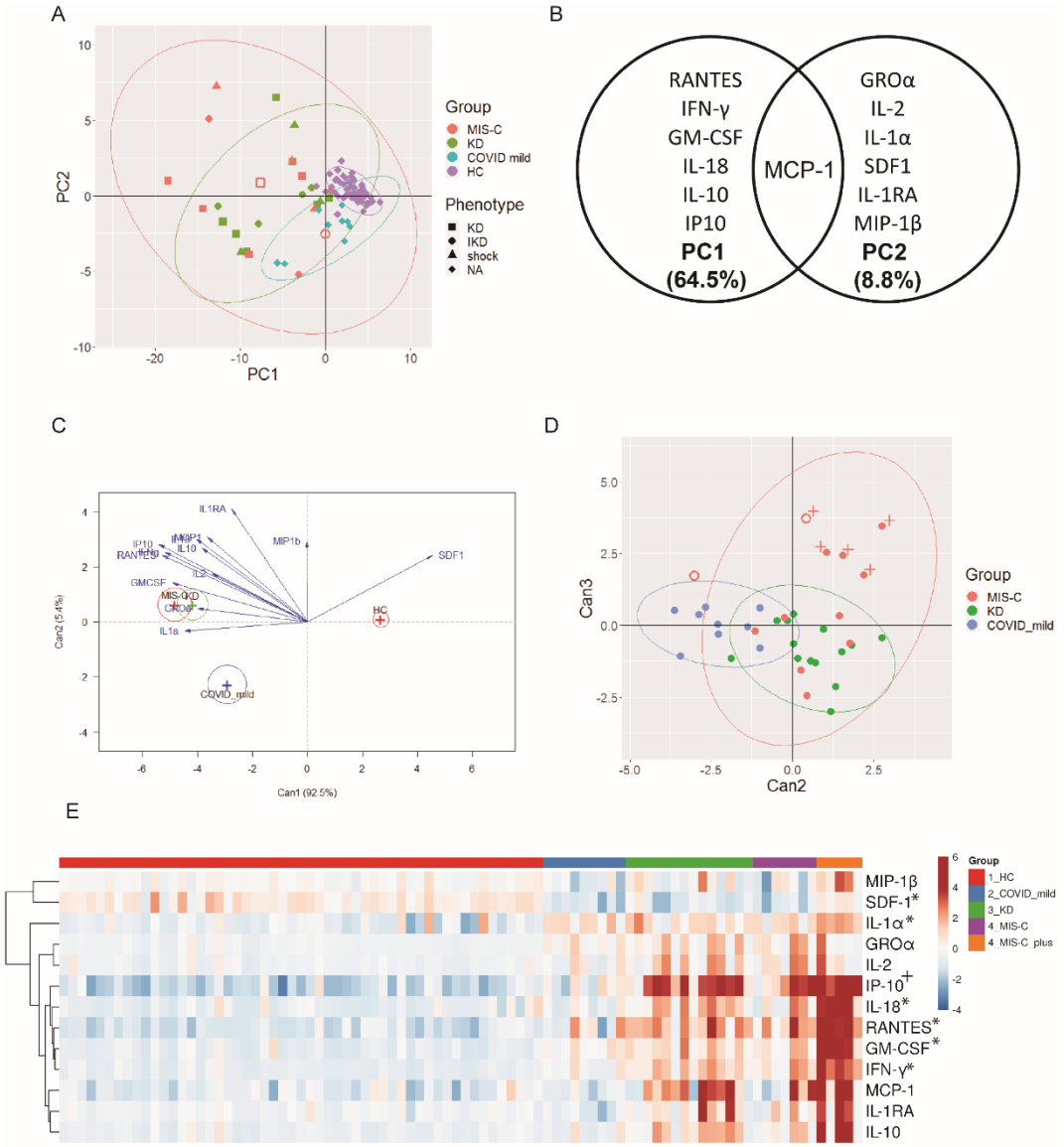

Figure 2. Cytokine profile of the different groups. Levels of 34 circulating cytokines were evaluated in serum or plasma. (A) Principal component analysis, every point represents one individual. (B) Total variance explained by principal component (PC) 1 and 2 and variables with higher scores. (C) Representation of canonical variants (Can) 1 and 2 of the linear discriminant analysis (LDA) built with the cytokines represented in "B". (D) Representation of Can2 and Can3 of the LDA (HC have been removed from the plot, not from the analysis). "+": subgroup of MIS-C patients differentiated from other MIS-C and KD patients (MIS-C^{plus}). Open symbols represent patients who previously received immunoglobulin treatment. E) Heatmap representing the selected cytokines (represented in panel B). Every column represents a patient. * identifies the cytokines with statically significant differences between KD+MIS-C and MIS-C^{plus}, "+"identifies cytokines with statically significant differences between MIS-C and MIS-C^{plus} and not with KD. Color gradient represents the z-score.

KD: Kawasaki disease pre-SARS-CoV-2 pandemics (n=14); MISC: multi inflammatory syndrome in children (n=13); COVID: pediatric patients with mild COVID-19 disease without MIS-C (n=9); HC: healthy controls (n=37, 53 samples)

	MIS-C	KD	COVID	HC
MIS-C (MIS-C^{plus})	33.33% (80%)	50.00% (20%)	16.67% (0%)	0.00% (0%)
KD	42.86%	42.86%	14.29%	0.00%
COVID	11.11%	22.22%	66.67%	0.00%
HC	0.00%	0.00%	0.00%	100.00%

Figure 3. Leave-one-out cross-validation of linear discriminant analysis model. Rows represent the pre-classified groups and columns the predicted categories after leave-one-out cross-validation. KD: Kawasaki disease pre-SARS-CoV-2 pandemics (n=14) ; MIS-C: multi inflammatory syndrome in children (n=13); COVID: pediatric patients with mild COVID-19 disease without MIS-C (n=9); HC: healthy controls (n=31; 53 samples).

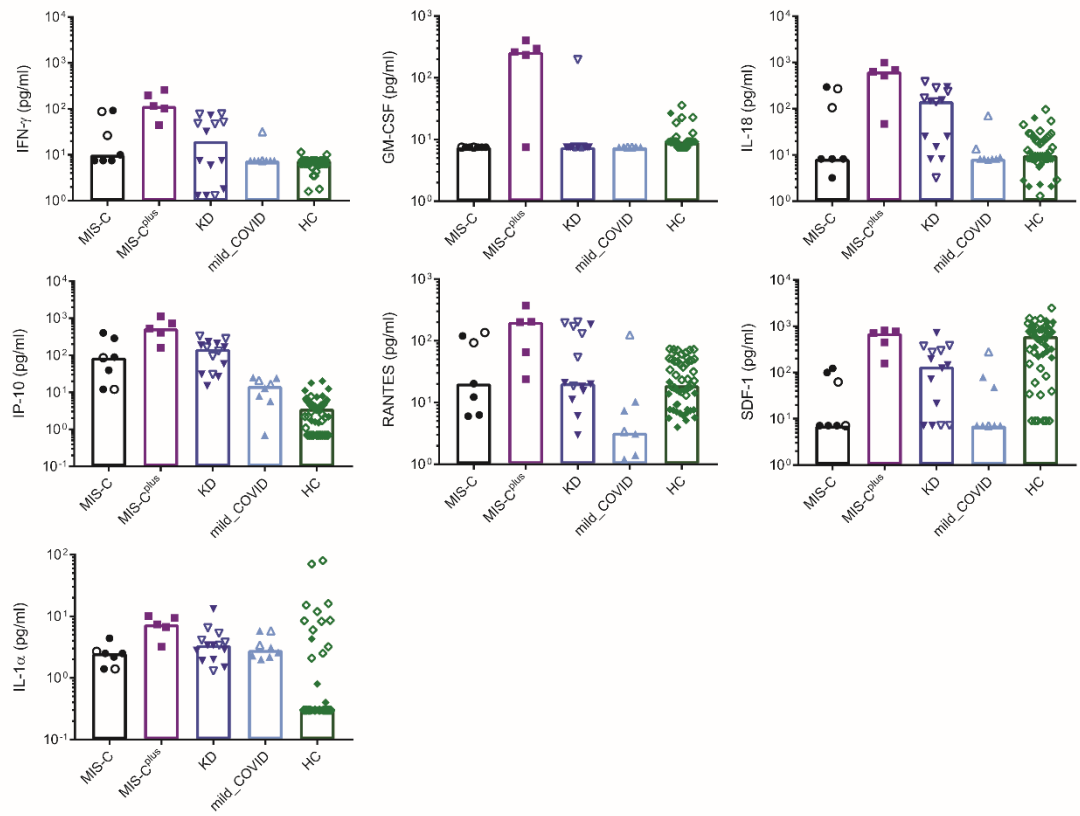

Figure 4. Quantitative circulating levels of selected cytokines. Quantitative levels of cytokines with significant differences between MIS-C (n=7) and MIS-C^{plus} (n=5) are shown. Open symbols represent plasma samples and filled symbols are serum samples. Bars represent median values. Described values for IFN-γ in 1) viral infections range from 7.7 to 33.4pg/ml(33), 2) suspected primary hemophagocytic syndrome with or without genetic confirmation range from 147.6 to >5000pg/ml(33) and a mean (95 confidence interval) of 905.7pg/ml (530.7–1280.6pg/ml)(35) and 3) patients with MAS in SoJIA mean (inter quartile range) of 15.4pg/ml (5.1-52.6pg/ml) (36).

KD: Kawasaki disease pre-SARS-CoV-2 pandemics (n=14); MISC: multi inflammatory syndrome in children (n=13); COVID: pediatric patients with mild COVID-19 disease without MIS-C (n=9); HC: healthy controls (n=37, 53 samples)

Table 1. Description of the study cohort: clinical data and SARS-CoV-2 related analytical data.

			MIS-C		KD		p	COVID	
Demographics	Sex[1]	Female , Male	7	7	6	8	1	5	4
	Age (years)	median, min-max	2.88	0.25-14	2.00	0.5-6	0.38	10	0.08-14
	Ethnicity[1]	North African (nº,%)	1	7.1%	3	21.4%		0	0.0%
		Latin (nº,%)	2	14.3%	2	14.3%		6	60.0%
		White (nº,%)	9	64.3%	8	57.1%	0.73	4	40.0%
		Asian (nº,%)	1	7.1%	1	7.1%		0	0.0%
		Black (nº,%)	1	7.1%	0	0.0%		0	0.0%
	Overweight	nº,%	1	7.1%	0	0.0%	0.31	2	20.0%
Symptoms	Fever	nº, %	14	100.0%	14	100.0%	-	6	60.0%
	Total Fever duration(days)	median, min-max	6.00	3-11	5.50	4-15	0.60	2.00	0-7
	Respiratory symptoms	nº,%	3	21.4%	2	14.3%	0.62	3	30.0%
	Gastrointestinal symptoms	nº,%	12	85.7%	6	42.9%	**0.02**	7	70.0%
	Neurologic symptoms	nº,%	5	35.7%	0	0.0%	**0.01**	1	10.0%
	Bilateral Conjunctivitis	nº,%	10	71.4%	12	85.7%	0.36	0	0.0%
	Oral mucosal changes	nº,%	10	71.4%	13	92.9%	0.14	0	0.0%
	Peripheral extremity changes	nº,%	9	64.3%	6	42.9%	0.26	0	0.0%
	Polymorphous rash	nº,%	11	78.6%	9	64.3%	0.40	2	20.0%
	Lymphadenopathy	nº,%	9	64.3%	7	50.0%	0.44	1	10.0%
	Diagnosis[2]	Complete KD	7	50%	6	42.9%			
		Incomplete KD	4	28.6%	6	42.9%	0.71		
		Shock	3	21.4%	2	14.3%			
	Aneurysms	nº,%	3	21.4%	1	7.1%	0.28		
	Cardiac dysfunction	nº,%	2	14.3%	0	0.0%	0.14		
	Vascular hyperpermeability	nº,%	7	50.0%	3	21.4%	0.12	0	0.0%
	Shock[3]	nº,%	3	21.4%	3	21.4%	1	0	0.0%
	Number of OSI[4] (0 to 8)	median, min-max	3.00	01-jun	3.00	01-abr	0.21		
	Highest level of care	Outpatient (nº,%)	0	0.0%	0	0.0%		4	40.0%
		Hospitalization (nº,%)	11	78.6%	12	85.7%		5	50.0%
		Hospitalization (high care) (nº,%)	0	0.0%	0	0.0%	0.36	1	10.0%
		ICU (ionotropics/ventilation) (nº,%)	3	21.4%	1	7.1%		0	0.0%
	Sequelae	Aneurysms (nº,%)	3	21.4%	1	7.1%	0.28	0	0.0%
Treatment	IVIG[5]	nº,%	12	85.7%	14	100.0%	0.14	0	0.0%
	IVIG second dose	nº,%	3	21.4%	1	7.1%	0.28	0	0.0%
	Systemic glucocorticoids	nº,%	8	57.1%	5	35.7%	0.25	1	10.0%
	IL-6 inhibitor	nº,%	0	0.0%	0	0.0%	-	0	0.0%
	Anticoagulation therapy	nº,%	12	85.7%	14	100.0%	-	1	10.0%
	Day of illness at treatment	median, min-max	5.00	0-9	5.00	1-8		5.00	5.00
	Treatment prior to cytokine evaluation	Antibiotic (nº,%)	9	64.3%	4	28.6%		2	20.0%
		IVIG (nº,%)	2	14.3%	0	0.0%		0	0.0%
	Lapse onset to cytokine evaluation (days)[6]	median, min-max	5.50	2-10	4.50	4-14	0.86	1.50	0-15
COVID-19	COVID contact	nº,%	3	21.4%			-	9	90.0%
	Positive PCR (NF[7])	Pos (nº,%)	4	28.6%			-	10	100.0%
	Positive PCR (stools)	Pos (nº,%)	2	40.0%			-	0	0.0%
	IgG- SARS-CoV-2	Pos (nº,%)	8	61.5%			-	8	80.0%
	IgA-SARS-CoV-2	Pos (nº,%)	6	46.2%			-	6	60.0%
		Indeterminable (nº,%)	1	7.7%			-	0	0.0%
	IgM-SARS-CoV-2	Pos (nº,%)	1	7.7%			-	6	60.0%

1. Classified by the investigators 2. 2017 AHA criteria; 3. Kanegaye Kawasaki shock criteria (45) 4. Organ systems involvement; 5. Intravenous immunoglobulins; 6. Days between onset of disease and sample extraction; 7. Nasopharyngeal. KD: Kawasaki disease pre-SARS-CoV-2 pandemics; MIS-C: multisystem inflammatory syndrome in children; COVID: pediatric patients with mild COVID-19 disease without MIS-C. IVIG: intravenous immunoglobulin; PCR: polymerase chain reaction; OSI: organ systems involvement; ICU: intense care unit.

Table 2. Cohort description: laboratory data.

		MIS-C	KD	COVID	KD *vs* MIS-C	KD *vs* COVID	MIS-C *vs* COVID
Hb (g/dL)	median. min-max. n	10.85 . 7.8-12.3 . 14/14	10.5 . 9.6 . 14/14	12.5 . 6.8-13.5 . 10/10	1	**0.026**	**0.036**
Platelets·10^3/mm^3 of blood	median. min-max. n	232,5 . 112-509 . 14/14	444 . 123-997 . 14/14	302,5 . 117-3380 . 10/10	0.035	**0.009**	0.625
Low Platelets	nº/total. %	4/14 . 28.6%	1/14 . 7.1%	1/10 . 10.0%	0.33		
Lymphocytes/mm^3	median. min-max. n	1950 . 400-10400 . 14/14	5550 . 1000-8200 . 14/14	2350 . 800-3300 . 10/10			
Lymphopenia	nº/total. %	9/12 . 75.0%	3/14 . 21.4%	5/10 . 50.0%	0.02		
Neutrophils/mm^3	median. min-max. n	6728.57 . 300-17300 . 14/14	10528 . 3286-16400 . 13/14	3050 . 500-7300 . 10/10	0.054	**0.001**	0.709
Neutrophilia	nº/total. %	6/14 . 42.9%	11/13 . 84.6%	2/10 . 20.0%	0.015		
Monocytes/mm^3	median. min-max. n	600 . 100-2700 . 14/14	600 . 212-1504 . 13/14		0.83		
Monocytosis	nº/total. %	7/14 . 50.0%	9/13 . 69.2%		0.44		
D-dimer (mg/L)	median. min-max. n	4.32 . 1.12-9.22 . 7/14		0.915 . 0.61-1.22 . 2/10			0.111
ESR mm/hour	median. min-max. n	18.5 . 30348.0 . 10/14	34.5 . 29252.0 . 14/14				
Altered ESRmm/hour	nº/total. %	5/10 . 50.0%	10/14 . 71.4%		0.4		
PCT (ng/ml)	median. min-max. n	2.28 . 0.04-6.74 . 14/14	0.6 . 0.08-4.42 . 14/14	0.02 . 0.01-0.53 . 8/10	0.401	**0.001**	**0.001**
Altered PCT	nº/total. %	10/14 . 71.4%	9/14 . 64.3%	1/8 . 12.5%	1		
CRP (mg/L)	median. min-max. n	156.25 . 33.2-364.0 . 14/14	116.9 . 36.9-407 . 14/14	1.4 . 0.2-63.6 . 9/10	0.874	**0**	**0**
Altered CRP	nº/total. %	14/14 . 100.0%	14/14 . 100.0%	3/9 . 33.3%	-		
Ferritin (µg/L)	median. min-max. n	375.5 . 66-2000 . 14/14	193.6 . 116-849.4 . 13/14	98.8 . 39.5-3545 . 5/10	0.65	0.566	0.823
Altered Ferritin	nº/total. %	10/14 . 71.4%	12/13 . 92.3%	2/5 . 40.0%	0.33		
NTPro-BNP (ng/L)	median. min-max. n	3102 . 131-22668 . 14/14	1445 . 80-6714 . 13/14		0.458		
Altered Pro-BNP	nº/total. %	14/14 . 100.0%	12/13 . 92.3%		0.48		
Na (mmol/L)	median. min-max. n	136.5 . 129-144 . 14/14	136 . 131*141.5 . 13/14	138 . 124-140 . 7/10	0.402	0.135	0.585
Altered NA	nº/total. %	5/14 . 35.7%	6/13 . 46.2%	1/10 . 10.0%	0.7		
ALT (U/L)	median. min-max. n	26.5 . 7-106 . 14/14	18 . 8-196 . 13/14	14.5 . 7-126 . 8/10	0.867	0.414	0.267
Altered ALT	nº/total. %	6/14 . 42.9%	5/13 . 38.5%	2/2 . 25.0%	1		
LDH (U/L)	median. min-max. n	673 . 402-891 . 14/14	557 . 289-1144 . 14/14	564 . 308-1037 . 7/10	0.482	0.636	0.128
Altered LDH	nº/total. %	5/14 . 35.7%	4/14 . 28.6%	3/7 . 42.9%	1		
Albumin (g/L)	median. min-max. n	35 . 20-46 . 12/14	35.5 . 23-42 . 14/14	.	0.595		
Altered albumin	nº/total. %	8/12 . 66.7%	8/14 . 57.1%		0.7		

KD: Kawasaki disease pre-SARS-CoV-2 pandemics; MIS-C: multisystem inflammatory syndrome in children; COVID: pediatric patients with mild COVID-19 disease without MIS-C. ND: not determined. y: years; Hb: hemoglobin; ESR: erythrocyte sedimentation rate; PCT: procalcitonin; CRP: C reactive protein; NT-ProBNP: NT-Pro-brain natriuretic peptide; ALT: alanine transaminase; LDH: lactate dehydrogenase. Na: sodium